COMPARATIVE INVESTIGATIONS OF THE MECHANICALLY ALLOYED and PRESSURELESS SINTERED Al–7 wt.% Si COMPOSITES REINFORCED WITH VARIOUS BORIDE PARTICLES

M.Sc. Mertdinç S.[1], M.Sc. Tekoğlu, E.[1], Dr. Ağaoğulları, D. [1], Prof. Dr. Öveçoğlu, M.L.[1]
Istanbul Technical University, Faculty of Chemical and Metallurgical Engineering, Department of Metallurgical and Materials Engineering, Particulate Materials Laboratories (PML), Ayazağa Campus, 34469 Maslak, Istanbul, Turkey[1]
mertdinc@itu.edu.tr

Abstract: *This study reports the milling time optimization of the Al-7 wt.% Si alloys by using planetary ball mill, the incorporation of 2 wt.% LaB_6, NbB_2, VB and TiB_2 particles into Al-7 wt.% Si matrix and the fabrication of composites using cold pressing and pressureless sintering. Mechanical alloying (MA) time carried out for 4, 8, 12, 16 and 20 h was optimized via crystallite size and phase determinations and microstructural investigations. 12 h was chosen as optimum MA time. Then, different particulate reinforcements were added to Al-7 wt.% Si matrix to constitute boride reinforced composites. All composite powder batches were also milled for 12 h, then compacted and sintered at 570°C for 5 h. Microstructural, physical and mechanical (hardness and wear volume loss) properties of these composites were performed. Hardness values of 120.8 ± 11.37 and 121.77 ± 19.02 were obtained for the LaB_6 and TiB_2 reinforced composites, respectively.*

Keywords: ALUMINIUM BASED COMPOSITES, PARTICULATE REINFORCEMENT, SINTERING, MICROSTRUCTURE

1. Introduction

Nowadays, metal matrix composites (MMCs) have wide range of application areas like aviation, defense and automotive [1–3]. Strength to weight ratio is an important parameter to improve the MMCs, so light metals are reinforced with ceramic particles that enable high strength to improve the properties of matrix metals or alloys [1,2,4,5]. Among the light-weight metals, Al-Si alloys draw a considerable interest due to their low density, low thermal expansion, high wear resistance, high stiffness, high corrosion resistances and good formability [3,6–8].

Although Al based composites were always produced with liquid-state production techniques, it is possible to produce this composites with solid-state processes [9,10]. Wettability of the reinforcement materials in the Al matrix is generally poor, so high energy milling can be used to produce homogeneous microstructures [10]. SPEX shaker mill, attritor ball mill, planetary ball mill, tumbler ball mill, vibratory ball mill are some types of mills that used for mechanical alloying (MA) in solid-state processes [10,11]. Amongst them, planetary ball mill is utilized for production of the milled powders in large quantities [11]. This is the main advantage of the planetary ball mill although SPEX shaker mill have 3 times higher rotation speed than that of planetary ball mill [11]. During the MA, powder particles are fractured, cold welded, fractured again and rewelded at high energy ball mill media. Therefore, powder particles are work hardened, particle sizes refine and composition homogeneity is achieved [11].

Up to now, aluminides, nitrides, carbides, oxides and borides were used as reinforcements for Al based MMCs due to their superior mechanical properties [12]. In this work, planetary ball mill were used for mechanical alloying and homogeneous dispersion of the reinforcement materials into the Al-7 wt.% Si matrix. LaB_6, NbB_2, VB and TiB_2 were chosen as reinforcement particulate materials for these experiments. Also, various boride reinforced Al-7 wt.% Si powders were milled for constant time, and they were pressed and sintered to produce boride reinforced composites. Mechanical, physical and microstructural properties of the boride reinforced composites were characterized.

2. Experimental Procedure

Al (Alfa Aesar™, 99.5 % purity, particle size ≤ 12 μm), Si (Alfa Aesar™, 99.99 % purity, particle size ≤ 20 μm), LaB_6 (Alfa Aesar™, 99 % purity, particle size ≤ 44 μm), NbB_2 (Alfa Aesar™, 99 % purity, particle size ≤ 44 μm), VB (Alfa Aesar™, 99 % purity, particle size ≤ 44 μm) and TiB_2 (Alfa Aesar™, 99 % purity, particle size ≤ 44 μm) powders were used as raw materials in the present study. As-blended Al-7 wt.% Si powders that were named as Al7Si were mechanically alloyed for 4, 8, 12, 16 and 20 h using a FRITSCH™ (400 rpm) planetary ball mill. Hardened steel vials (500 ml) and balls (ϕ 6 mm) were used, and ball-to-powder weight ratio was chosen as 7/1. Vials filled with powder batches were sealed inside a Plaslabs™ glove box (under Ar gas supplied by Linde™ with 99.999 % purity) to prevent the oxidation. MA'd powders were characterized by Bruker™ D8 Advanced Series X-ray diffractometer (XRD) with CuK_α (λ=1.5406 Å) radiation, 35 kV and 40 mA operating conditions to determine the crystalline phases. Also, Bruker™-AXS TOPAS 4.2 software was used to crystallite size and lattice deformation calculations. Then, morphologies of the powders were characterized via JEOL™ JCM-6000Plus NeoScope scanning electron microscope (SEM) coupled with energy dispersive spectroscopy (EDS).

After the morphological characterizations, optimum MA time was determined and 2 wt.% different types of boride reinforcements (LaB_6, NbB_2, VB and TiB_2) were added into Al7Si matrix one by one. 12 h MA'd powders were compacted using a MSE™ MP-0710 one-action hydraulic press under 450 MPa uniaxial pressure. Each compacted sample was debinded in a Protherm™ tube furnace under Ar gas flow at 420°C for 2 h with 2°C/min heating and cooling rate. Debinded bodies were sintered at 570°C in a Linn™ HT-1800 furnace under inert Ar atmosphere for 5 h (heating and cooling rate was 10°C/min).

Microstructural characterizations of the sintered samples were carried out using XRD and SEM. Density measurements of the sintered compacts were carried out using Archimedes method. Then, Vickers microhardness tests were conducted on the sintered samples using a Shimadzu™ HMV microhardness tester under a load of 25 g for 10 s. Result for each sample is the arithmetic mean of 10 successive indentations and standard deviations. Wear tests were carried out Tribotechnic™ oscillating tribotester by using 100Cr6 steel balls (6 mm), 3 N applied force, 5 mm/s sliding speed and 25,000 mm total sliding distance. Morphologies of the worn surfaces were examined with SEM. Besides, compression tests were performed to determine the compression strength, yield strength and strain at Shimadzu™ Autograph AGS-J at loading rate of 0.18 mm/min.

3. Results and Discussion

First of all, Al7Si matrix alloy was MA'd for different durations, and phase and morphology investigations were conducted to determine the optimum MA duration. Fig. 1(a)-(e) show the XRD patterns of the Al7Si powders MA'd with different durations (4, 8, 12, 16 and 20 h). XRD patterns of the powders displayed only the Al and Si phases. Intermetallic phase formation and contamination

were not detected in the powders even after 20 h milling (within the detection sensitivity of the diffractometer).

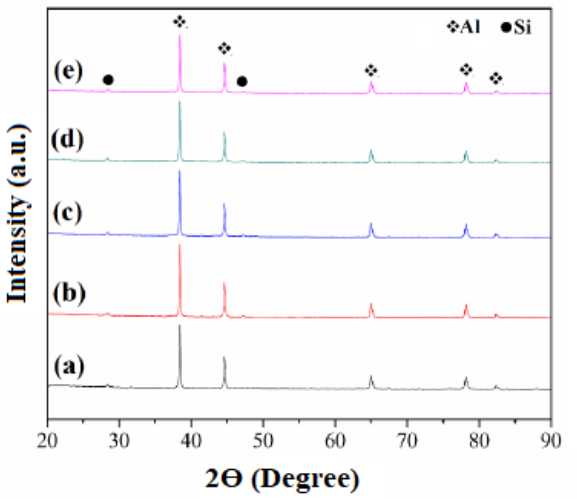

Fig. 1: *XRD patterns of the Al7Si powders MA'd for 4 h (a), 8 h (b), 12 h (c), 16 h (d) and 20 h (e).*

Calculated average crystallite sizes and average lattice deformations of the MA'd (for 4, 8, 12, 16 and 20 h) Al7Si powders are given at Table 1. Average crystallite sizes of the powders were reduced and their lattice strains were increased with increasing MA time. Because, plastic deformation during milling provided the lattice strain increment [13].

Table 2: *Average crystallite sizes and lattice deformations of the MA'd (for 4, 8, 12, 16 and 20 h) Al7Si powders.*

MA time [h]	Average crystallite size [nm]	Average lattice strain [%]
4	88.2	0.118
8	73.7	0.189
12	62.4	0.221
16	56.9	0.299
20	48.7	0.345

SEM micrographs of Al7Si powders MA'd for 4, 8, 12, 16 and 20 h are presented at Fig. 2 (a)-(e), respectively. 4 h MA'd powder get flattened due to the ball-to-powder collisions. Besides, 8 and 12 h MA'd powders have equiaxed and agglomerated particle morphologies. However, 16 and 20 h MA'd powders get flattened again. Moreover, flattened particles cause crack and porosity formation after pressing and sintering [11]. Therefore, optimum MA duration was selected as 12 h to obtain homogeneous particle size formation.

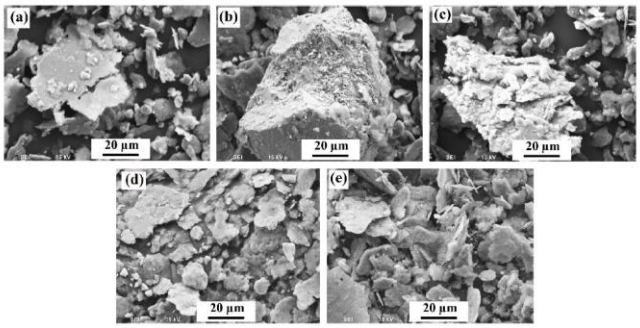

Fig. 2: *SEM micrographs of the Al7Si powders MA'd for 4 h (a), 8 h (b), 12 h (c), 16 h (d) and 20 h (e).*

After the MA time optimization, all different reinforcement particles were added to Al7Si and these blends were MA'd for 12 h to constitute Al7Si-2LaB_6, Al7Si-2NbB_2, Al7Si-2VB and Al7Si-2TiB_2 powders. Microstructural and phase characterizations were performed for the MA'd powders, then microstructural, physical and mechanical properties of the sintered bodies were characterized after pressing and sintering of these MA'd powders.

Fig. 3(a)-(d) show the XRD patterns of the Al7Si-2LaB_6, Al7Si-2NbB_2, Al7Si-2VB and Al7Si-2TiB_2 powders, respectively. Only Al, Si and boride phases were detected. There is not intermetallic phase formation between the Al, Si and reinforcement particles.

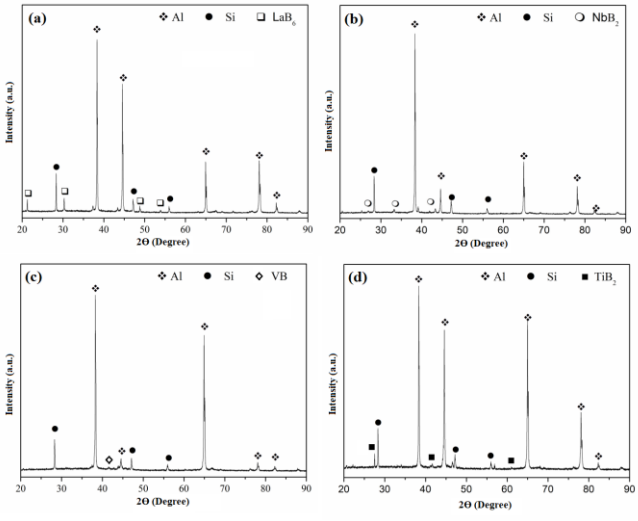

Fig. 3: *XRD patterns of the boride reinforced Al7Si powders MA'd for 12 h: Al7Si-2LaB_6 (a), Al7Si-2NbB_2 (b), Al7Si-2VB (c), Al7Si-2TiB_2 (d).*

SEM micrographs of the boride reinforced Al7Si powders MA'd for 12 h (Al7Si-2LaB_6, Al7Si-2NbB_2, Al7Si-2VB and Al7Si-2TiB_2 powders) are given in Fig. 4(a)-(d). Hard and brittle reinforcement particles caused the fracturing of the matrix material during milling. Flaky shaped particles were seen in Fig. 4 for all reinforced powders. However, the fracturing is seen obviously in the NbB_2 and TiB_2 reinforced powders (Fig. 4(b) and (d)).

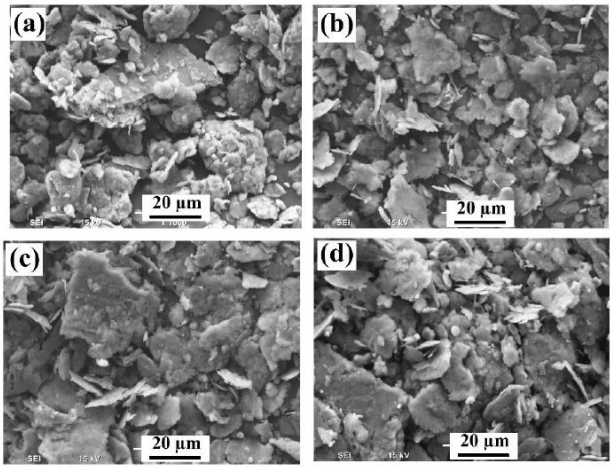

Fig. 4: *SEM micrographs the boride reinforced Al7Si powders MA'd for 12 h: Al7Si-2LaB_6 (a), Al7Si-2NbB_2 (b), Al7Si-2VB (c), Al7Si-2TiB_2.*

Each powder was compacted and sintered. After that, microstructural, physical and mechanical properties of the sintered compacts were determined via characterization investigations and their results are explained below.

OM images of the sintered compacts are given in Fig. 5 (a)-(d) for Al7Si-2LaB_6, Al7Si-2NbB_2, Al7Si-2VB and Al7Si-2TiB_2 samples. Si (dark regions) distributed homogeneously into the Al matrix. Also, particulate reinforcements distributed homogeneously via MA.

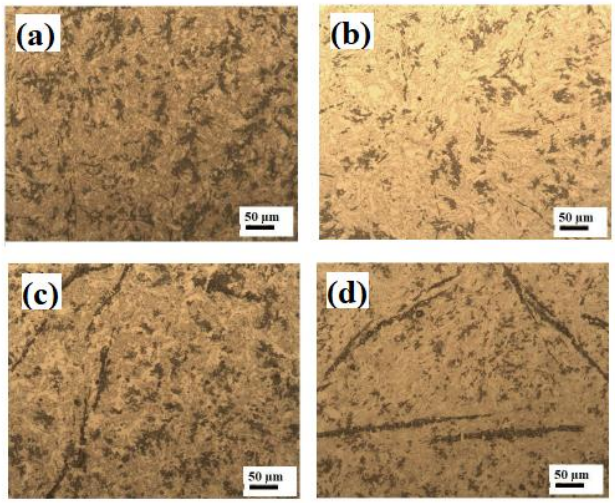

Fig. 5: *OM images of the sintered boride reinforced Al7Si samples: Al7Si-2LaB_6 (a), Al7Si-2NbB_2 (b), Al7Si-2VB (c), Al7Si-2TiB_2 (d).*

Theoretical density and Archimedes density results are presented at Table 2. The highest relative density value was reached with LaB_6 reinforcement and the lowest relative density value was obtained with TiB_2 reinforcement. Densities of the samples related with the interfacial area between the reinforcement and matrix material. If the reinforcement particles inhibit the diffusion during solid-state sintering, lower densities enabled than the theoretical densities [8]. Otherwise, densities of the reinforced samples are low due to the flaky shaped morphologies of the milled powders. These flaky microstructures affect negatively the compaction and dense bodies were not produced.

Table 2: *Density measurements of the sintered samples.*

Sample	Theoretical Density (g/cm^3)	Archimedes Density (g/cm^3)	Relative Density (g/cm^3)
Al7Si	2.672	2.62	88.18
Al7Si-2LaB_6	2.690	2.66	88.90
Al7Si-2NbB_2	2.672	2.65	87.96
Al7Si-2VB	2.696	2.64	87.89
Al7Si-2TiB_2	2.692	2.58	86.01

Table 3 shows the average Vickers microhardness results taken from the 10 successful indentations for each sample. Hardness of the MA'd and sintered composites with various reinforcements are higher than the hardness of the MA'd and sintered Al-Si matrix alloy. The Vickers microhardness value of the VB reinforced composite is the highest value amongst all samples. Besides, wear volume tests were conducted for all reinforced samples. VB reinforced composite has the lowest wear volume loss. Therefore, VB reinforcement improve the wear resistance and microhardness of the matrix.

Table 3: *Microhardness measurements and wear volume losses of the sintered samples.*

Sample	Vickers Microhardness (HV)	Standard Deviation	Wear volume loss (mm^3)
Al7Si	104.7	±20.1	-
Al7Si-2LaB_6	120.8	±11.3	0.007
Al7Si-2NbB_2	114.9	±14.6	0.012
Al7Si-2VB	135	±28.4	0.005
Al7Si-2TiB_2	121.7	±19.0	0.010

Wear tracks of the Al7Si-2LaB_6, Al7Si-2NbB_2, Al7Si-2VB, Al7Si-2TiB_2 sintered compacts are presented in Fig. 6(a)-(d). Abrasive grooves were observed at these SEM images. Wear track of the Al7Si-2VB sample is the narrowest one. These wear track images are in good agreement with the wear volume loss results.

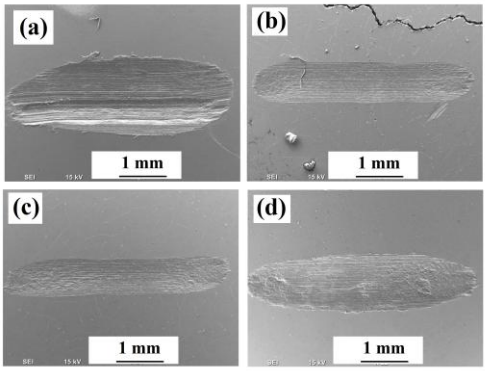

Fig. 6*: SEM images of the wear tracks taken from the sintered samples: Al7Si-2LaB_6 (a), Al7Si-2NbB_2 (b), Al7Si-2VB (c), Al7Si-2TiB_2.*

Compression strength, yield strength, elastic strain and strain of the all sintered samples are listed at Table 4. The highest yield strength was obtained for the TiB_2 reinforced composite whereas the highest compression strength was obtained for the LaB_6 reinforced one. Also, elastic strains of the composites were not high; this situation is probably arisen from the flaky shaped reinforced and milled powders. These types of hard and brittle reinforcements resulted in a weak bonding in the ductile matrix and mechanical properties were not found as so high.

Table 4: *Compression strength, yield strength, elastic strain and strain of the sintered samples.*

Sample	Yield Strength (MPa)	Compression Strength (MPa)	Elastic Strain (%)	Total Strain (%)
Al7Si-2LaB_6	103	164	0.37	2.18
Al7Si-2NbB_2	101	152	0.27	0.60
Al7Si-2VB	93	140	0.31	0.66
Al7Si-2TiB_2	119	142	0.42	0.68

4. Conclusion

In this study, effects of the various types of boride reinforcements into the Al7Si matrix were examined. The usage of the planetary ball mill in mechanical alloying applications was also investigated. Based on the characterization investigations, results can be summarized as below:

- Al7Si matrix powders were milled for different durations. Although, crystallite sizes reduced with increasing MA time, particles were started to be flattened after 12 h of MA. Therefore, optimum MA time was chosen as 12 h.
- Among the sintered samples, the highest relative density was obtained for the Al7Si-2LaB_6 sample
- Among the sintered samples, the highest hardness and wear resistance were obtained for the Al7Si-2VB sample. Besides, Al7Si-2TiB_2 composite has the highest yield strength.

References

[1] D. Garbiec, M. Jurczyk, N. Levintant-Zayonts, T. Mościcki, Properties of Al-Al<inf>2</inf>O<inf>3</inf> composites synthesized by spark plasma sintering method, Archives of Civil and Mechanical Engineering. 15 (2015) 933–939. doi:10.1016/j.acme.2015.02.004.

[2] M. Hossein-Zadeh, M. Razavi, M. Safa, A. Abdollahi, O. Mirzaee, Synthesis and structural evolution of vanadium carbide in nano scale during mechanical alloying, Journal

of King Saud University - Engineering Sciences. 28 (2016) 207–212. doi:10.1016/j.jksues.2014.03.010.

[3] S.Q. Wu, H.Z. Wang, S.C. Tjong, Mechanical and wear behavior of an Al/Si alloy metal-matrix composite reinforced with aluminosilicate fiber, Composites Science and Technology. 56 (1996) 1261–1270. doi:10.1016/S0266-3538(96)00085-1.

[4] A.K. Bodukuri, K. Eswaraiah, K. Rajendar, V. Sampath, Fabrication of Al–SiC–B4C metal matrix composite by powder metallurgy technique and evaluating mechanical properties, Perspectives in Science. 8 (2016) 428–431. doi:10.1016/j.pisc.2016.04.096.

[5] K.D. Woo, D.L. Zhang, Fabrication of Al-7wt%Si-0.4wt%Mg/SiC nanocomposite powders and bulk nanocomposites by high energy ball milling and powder metallurgy, Current Applied Physics. 4 (2004) 175–178. doi:10.1016/j.cap.2003.11.002.

[6] W.K. Kang, F. Yilmaz, H.S. Kim, J.M. Koo, S.J. Hong, Fabrication of Al-20 wt%Si powder using scrap Si by ultra high-energy milling process, Journal of Alloys and Compounds. 536 (2012) S45–S49. doi:10.1016/j.jallcom.2012.01.106.

[7] W.S. Miller, L. Zhuang, J. Bottema, A.J. Wittebrood, P. De Smet, A. Haszler, A. Vieregge, Recent development in aluminium alloys for the automotive industry, Materials Science and Engineering: A. 280 (2000) 37–49. doi:10.1016/S0921-5093(99)00653-X.

[8] E. Tekoğlu, D. Ağaoğulları, S. Mertdinç, A.H. Paksoy, M.L. Öveçoğlu, Microstructural characterizations and mechanical properties of NbB2and VB particulate-reinforced eutectic Al-12.6 wt% Si composites via powder metallurgy method, Advanced Powder Technology. (2018). doi:10.1016/j.apt.2018.05.013.

[9] R. Flores-Campos, D.C. Mendoza-Ruiz, P. Amézaga-Madrid, I. Estrada-Guel, M. Miki-Yoshida, J.M. Herrera-Ramírez, R. Martínez-Sánchez, Microstructural and mechanical characterization in 7075 aluminum alloy reinforced by silver nanoparticles dispersion, Journal of Alloys and Compounds. 495 (2010) 394–398. doi:10.1016/j.jallcom.2009.10.209.

[10] M.S. El-Eskandarany, Introduction, Mechanical Alloying. (2015) 1–12. doi:10.1016/B978-1-4557-7752-5.00001-2.

[11] C. Suryanarayana, Mechanical alloying and milling, Progress in Materials Science. 46 (2001) 1–184. doi:10.1016/S0079-6425(99)00010-9.

[12] Ö. Balci, D. Ağaoğullari, H. Gökçe, I. Duman, M.L. Öveçoğlu, Influence of TiB2 particle size on the microstructure and properties of Al matrix composites prepared via mechanical alloying and pressureless sintering, Journal of Alloys and Compounds. 586 (2014) s78–s84. doi:10.1016/j.jallcom.2013.03.007.

[13] J. Milligan, R. Vintila, M. Brochu, Nanocrystalline eutectic Al-Si alloy produced by cryomilling, Materials Science and Engineering A. 508 (2009) 43–49. doi:10.1016/j.msea.2008.12.017.

Acknowledgements

This study was supported by The Scientific and Technological Research Council of Turkey (TUBITAK) with the project number of 214M093. The authors would like to express their appreciations to Yakup Yürektürk for his help in mechanical tests.